Structural models for room temperature stable radiation-induced centres in zircon

1999 J. Phys.: Condens. Matter 11 8579

(http://iopscience.iop.org/0953-8984/11/43/321)

J. Phys.: Condens. Matter **11** (1999) 8579–8589. Printed in the UK PII: S0953-8984(99)04490-2

Structural models for room temperature stable radiation-induced centres in zircon

R F C Claridge†, W C Tennant†, S Schweizer‡ and J-M Spaeth‡

† Chemistry Department, University of Canterbury, Private Bag 4800, Christchurch, New Zealand
‡ Fachbereich Physik, Universität-GH Paderborn, D-33095 Paderborn, Germany

Received 19 May 1999

Abstract. Several x-ray-induced paramagnetic defects stable to room temperature are generated when $ZrSiO_4$ single crystals are irradiated at 77 K. In a previous EPR investigation, two of these stable defects, labelled C and Z, were described as 'unusual' and were thought to be coupled to each other by a ferrimagnetic interaction of about 23 cm^{-1} at low temperature. New EPR experiments down to 4.2 K on recently synthesized single crystals have revealed that C and Z are not correlated. The Z centre is now shown to be Cr^{3+} in an Si site and has an unusually high zero field splitting constant of $\sim$1.5 T, possibly caused by the strong crystal field due to the two Zr^{4+} ions along the *c*-axis. The C centre is proposed to be an oxygen hole centre where the oxygen 2p hole orbital is oriented towards a nearest neighbour Zr^{4+} vacancy which stabilizes the hole by Coulomb forces thus explaining the high thermal stability of the centre. The hyperfine interaction with one ^{29}Si and one ^{91}Zr neighbour is explained including exchange polarization effects and the near isotropic *g*-values by near complete orbital quenching.

1. Introduction

X-irradiation at 77 K of a synthetic zircon single crystal ($ZrSiO_4$) generates a number of thermally unstable paramagnetic defects. Several of these have been studied previously by electron paramagnetic resonance (EPR) [1–3]. After annealing the crystal to room temperature and recooling to low temperature three major defect centres are observed: a Ti^{3+} defect (d^1 electronic structure, [3]) and two other centres which were labelled C and Z, the structural models of which remained unclear. These centres persist unchanged when the crystals are stored for several months at room temperature. This stability indicates that they are deep traps and suggests that the structures must be simple. When analysed separately the C and Z had other features that were puzzling. The *g*-factor for the C centre is 1.9993 and essentially isotropic in a tetragonal crystal where all other centres hitherto studied were of uniaxial or lower symmetry [1–3]. In contrast, the Z centre is highly anisotropic with apparent *g*-factors between 1.9991 and 3.9118 [4]. The two centres, C and Z, seemed to be not independent of one another. From an apparently identical microwave saturation behaviour above 14 K and the coincidence of the *g*-values along the *c*-axis it was proposed that they were part of a ferrimagnetically coupled triradical system with a scalar coupling constant of 23 cm^{-1}. At higher temperatures this coupling was assumed to be broken by thermal activation. Because of this strange behaviour the pair of defects, C and Z, were called an 'unusual centre' [4].

We now report on further EPR experiments on the Z centre, and a more detailed study of the microwave saturation behaviour of both C and Z centres below 20 K. Structural models

0953-8984/99/438579+11$30.00

for both centres which explain the observed EPR data as well as their thermal stability are presented. It turned out that these centres are independent and not unusually coupled.

It is proposed that the Z centre is a Cr^{3+} ion on an Si site and that the C centre is an oxygen hole centre whereby the hole is stabilized by a nearest neighbour Zr^{4+} vacancy.

2. Experiment

The zircon crystal used in the original C and Z centre experiments was obtained from Aerospace Corp and had been grown from molten Li_2SiO_3–MoO_3 by the method described by Chase and Osmer [5]. The crystal was cut accurately to a parallelepiped with the faces parallel to the crystallographic axes a, b and c of the tetragonal (space group $I4_1/amd$) crystal system. Although this crystal was nominally undoped, numerous paramagnetic centres have been observed in it, several of which have been described [1–4]. The number and nature of the paramagnetic defects depend on the previous heat treatment of the crystal, the type and temperature of irradiation to which it is subjected, any subsequent heating and the temperature at which the EPR measurements are made. More recently smaller crystals have been grown in the University of Canterbury crystal growth laboratory using the same flux-growth method, again nominally without any added impurities. These smaller crystals all had well developed faces. The mounting of the crystals for irradiation and details of angular dependence measurements of the spectra are given in [4].

The crystals were irradiated at 77 K with x-rays from a tungsten tube (50 mA at 50 kV for 30 min). When examined at ∼15 K without warming the EPR spectra showed the presence of the two prominent centres, the $Zr^{3+}(\alpha)$ and the $[AlO_4]^0$ hole centre, along with some minor centres. The crystals were then annealed to room temperature to allow the thermally unstable centres to decay and then recooled. The EPR measurements described in [4] were performed on a modified Varian E12 X-band spectrometer at ∼15 K using a closed cycle liquid helium refrigeration system at the University of Canterbury. Further measurements between 4.2 K and room temperature were made in a custom-built, computer-controlled X-band EPR/ENDOR spectrometer at the University of Paderborn using a variable temperature cryostat. Attempts to measure ENDOR spectra of the C and Z centres were not successful, probably due to insufficient signal-to-noise ratio in the EPR spectra. For further details of the precise measurements of the angular dependence of the EPR spectra, necessary because of the very narrow lines (peak-to-peak linewidth 0.02 mT and independent of crystal orientation), see [4].

3. Experimental results

The original observation of the C centre [4] has been confirmed in all the new undoped crystals. It consists of an intense isotropic central line flanked by several small hyperfine lines (see figure 1 of [4]). The small hyperfine lines were analysed in [4] to be due to interactions with one ^{29}Si neighbour ($I = 1/2$, relative abundance 4.67%) and one ^{91}Zr neighbour ($I = 5/2$, relative abundance 11.2%). The g-factors and the hf matrices are reproduced from [4] in table 1 to enable a discussion of models of the C centre (see section 4).

As EPR spectra of irradiated crystals from different growth runs were examined it was observed that the intensity of the Z centre varied considerably, although all crystals were nominally undoped. The fact that the relative intensity of C and Z varied with different growth batches provided a clear indication that the two centres were not coupled but independent and that an alternative model must be sought. Figure 1 shows the EPR spectrum in one such

Table 1. Spin Hamiltonian (SH) parameters for the C centre (reproduced from [4])[a].

	Matrix **Y**			k	Principal value, Y_k	Principal direction[b] θ_k (°)	ϕ_k (°)
	1.99939(1)	0	0	1	1.99939(1)	90	0
$\boldsymbol{g}$		1.99937(1)	0	2	1.99937(1)	90	90
			1.99924(1)	3	1.99924(1)	0	0
^{29}Si ($I = 1/2$) superhyperfine interaction							
	0.5474(8)	0	0.0649(5)	1	0.6494(5)	147.5(2)	180
$\mathbf{A}/g_e\beta_e$		0.5023(8)	0	2	0.5061(8)	57.5(2)	180
(mT)			0.6081(3)	3	0.5023(8)	90	90
^{91}Zr ($I = 5/2$) superhyperfine interaction							
	0.0413(13)	0	0	1	0.0635(6)	30.2(2.4)	90
$\mathbf{A}/g_e\beta_e$		0.0540(12)	0.0055(4)	2	0.0508(9)	120.2(2.4)	90
(mT)			0.0603(3)	3	0.0413(13)	90	0

[a] Error estimates in parentheses.
[b] Angle θ measured from $\boldsymbol{c}$ and angle ϕ in an anticlockwise direction from $\boldsymbol{a}$.

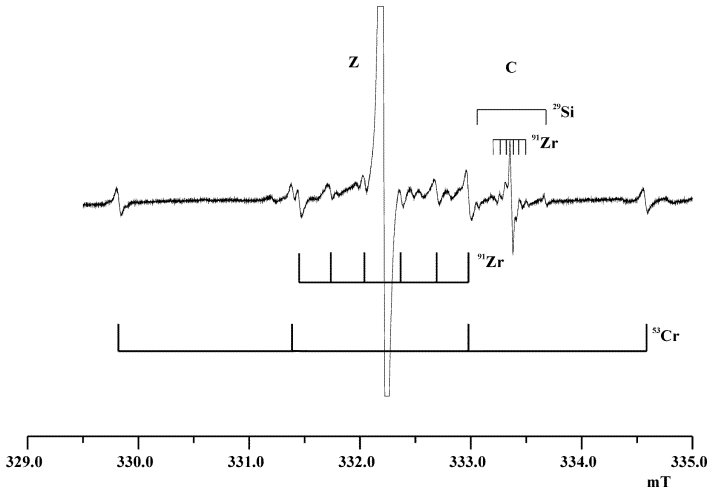

Figure 1. EPR spectrum showing the C and Z centres. The magnetic field has been rotated 3.0° away from the c-axis. The superhyperfine lines due to ^{29}Si ($I = 1/2$, 4.67%) and ^{91}Zr ($I = 5/2$, 11.2%) on the C centre, and the hyperfine lines due to ^{53}Cr ($I = 3/2$, 9.50%) and the superhyperfine lines due to ^{91}Zr on the Z centre are marked.

crystal with a large signal due to the Z centre measured for a magnetic field 3° away from the c-axis. The previously observed ^{29}Si doublet and the ^{91}Zr sextet hyperfine lines of the C centre are marked. Now, however, resolved hf splitting on the Z centre can be seen. Two sets of hf lines are marked: a quartet ($A = 1.5$ mT) due to a nucleus with $I = 3/2$, and a sextet of lines ($A = 1.18$ mT) due to a nuclear spin with $I = 5/2$. The intensity of the hf lines of the quartet relative to the central line is (2.5 ± 0.5):100 which identifies the hf quartet to be due to ^{53}Cr ($I = 3/2$ and relative abundance 9.5%). The expected ratio of line intensities for ^{53}Cr is 2.95:100. There is no other $I = 3/2$ isotope which would cause anything near to this intensity ratio. Thus the Z centre is basically a Cr impurity and, from the observed g anisotropy together with some aspects of the hfs, we believe it to be Cr^{3+} (see next paragraph

Table 2. SH parameters for the Z centre fitted to a quartet, $S = 3/2$, system[a].

Matrix **Y**				k	Principal value, Y_k	Principal direction[b] θ_k (°)	ϕ_k (°)
	1.9564(3)	0	0	1	1.9993(1)	0.5(1)	270
$\boldsymbol{g}$		1.9573(2)	−0.0004(1)	2	1.9573(2)	89.5(1)	90
			1.9993(1)	3	1.9564(3)	90	0
	1.51(31)	0	0	1	−3.03(62)	0	0
$\mathbf{D}/g_e\beta_e$		1.51(31)	0	2	1.51(31)	90	0
(T)			−3.03(62)	3	1.51(31)	90	90
^{53}Cr ($I = 3/2$) hyperfine interaction							
	1.58(1)	0	0	1	1.58(1)	0	0
$\mathbf{A}/g_e\beta_e$		1.16(1)	0	2	1.16(1)	90	0
(mT)			1.16(1)	3	1.16(1)	90	90
^{91}Zr ($I = 5/2$) superhyperfine interaction							
	0.31(2)	0	0	1	0.31(2)	0	90
$\mathbf{A}/g_e\beta_e$		0.24(2)	0	2	0.24(2)	90	0
(mT)			0.24(2)	3	0.24(2)	90	90

[a] Error estimates in parentheses.
[b] Angle θ measured from $\boldsymbol{c}$ and angle ϕ in an anticlockwise direction from $\boldsymbol{a}$.

and proposed structural model in the discussion section). In the previous measurements the Z centre EPR intensity was not high enough to resolve the weak ^{53}Cr hf lines. The sextet of lines had been observed before [4] but was too weak to establish a reliable intensity ratio. This has now been possible giving the ratio (4.0 ± 0.5):100 indicating that we have interaction with two ^{91}Zr neighbours (expected ratio 4.12:100). The angular dependence of the Z centre shows no site splitting although the linewidth increases markedly as the magnetic field is rotated away from the c-axis.

As detailed in [4] the data for the Z centre can be analysed in two equivalent ways, either as a spin quartet, $S = 3/2$ (see table 2 as reproduced from [4]), or to an effective spin $S' = \frac{1}{2}$. Assuming the latter, an almost uniaxial g-matrix with $g_\parallel = 1.9991$ and $g_\perp = 3.9118$ has been determined [4]. The hyperfine principal values in this fit are, in units $1/g_e\beta_e$, $A_\parallel = 1.56$ mT and $A_\perp = 2.32$ mT. As detailed by Pilbrow [6], these results are those expected from transitions *within* one doublet of a spin quartet system when $|D| \gg g_e\beta_e B$. For D positive the transition is within the upper doublet; the lower doublet produces effective g-values $g_\parallel = 6$ and $g_\perp = 0$ which, as noted in [4], is EPR silent at X-band frequencies. From [6] the effective A-values in the $S' = \frac{1}{2}$ doublet can be calculated $A'_\parallel = (g'_\parallel/g_\parallel)A_\parallel = 1.58$ mT and $A'_\perp = (g'_\perp/g_\perp)A_\perp = 2.32$ mT almost exactly as obtained in the $S' = \frac{1}{2}$ fit.

The $S = 3/2$ analysis of the angular dependence (see table 2) yields a large uniaxial zero field splitting term, D $(=3B_2^0)$, and an almost uniaxial g-matrix about the c-axis with principal values 1.9993, 1.9573 and 1.9564 close to other Cr^{3+} values. Recent synthesis of a zircon crystal with Cr_2O_3 added to the melt resulted in an identical EPR spectrum to that of the Z centre confirming the assumption that it arises from Cr^{3+} with $S = 3/2$.

Using a crystal in which the EPR intensities for both C and Z centres were comparable a careful investigation of the saturation behaviour as a function of microwave power and temperature down to low temperature was carried out. Figure 2 shows the results for low microwave power in a semi-log plot of the EPR intensity against temperature. The saturation

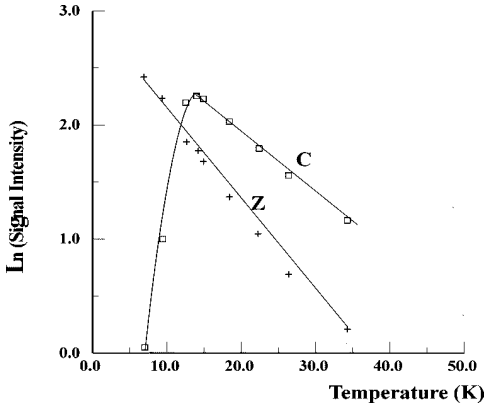

Figure 2. Temperature dependence of the EPR line intensity of C and Z centres.

behaviour of the C and Z centres are similar above about 14 K where all previous measurements were made. Below 14 K the intensity of the C centre decreases rapidly whereas that of Z does not, indicating that the spin–lattice relaxation times, T_1, for the two centres are different. Altogether these observations show that C and Z are independent centres and not coupled to each other. New models are now required.

4. Discussion

4.1. Structural model for the C centre

The puzzling properties of the C centre are that hf interaction with one Si and one Zr was found, the latter being an order of magnitude smaller than the former, and both being anisotropic whereas the g-matrix for the centre is almost isotropic with g-values near the free-electron values. The hf interaction matrices given in [4] are reproduced in table 1. From these data the isotropic hyperfine constant, a/h and the anisotropic hf constants, b/h and b'/h, which are related to the principal values of the hyperfine tensor **A** by $A_{xx} = a - b + b'$, $A_{yy} = a - b - b'$ and $A_{zz} = a + 2b$ can be derived (table 3). The term b'/h describes the deviation of the hf interaction from uniaxial symmetry (see e.g. [7]). The significance of these hf interaction constants will be discussed below.

Table 3. Theoretical ^{29}Si hf interaction constants (in MHz) assuming the regular O^-–Si^{4+} separation of 162 pm. α is the angle between the 2p hole axis and the O^-–Si^{4+} direction. The negative sign of g_n (^{29}Si) is taken into account for the calculation of the interaction constants. $b_{overlap}$ is the contribution of the component of the oxygen 2p hole orbital in the connection line O^-–Si^{4+}.

α (°)	a_{pol}/h	$a_{overlap}/h$	a_{theo}/h	a_{exp}/h	
90	26.3			26.3	±15.6
99	25.7	−5.9	19.8		
	b_{pol}/h	$b_{overlap}/h$	b_{dd}/h	b_{theo}/h	b_{exp}/h
90	5.3		−3.7	1.6	±0.78
99	5.2	−0.8	−3.6	0.8	

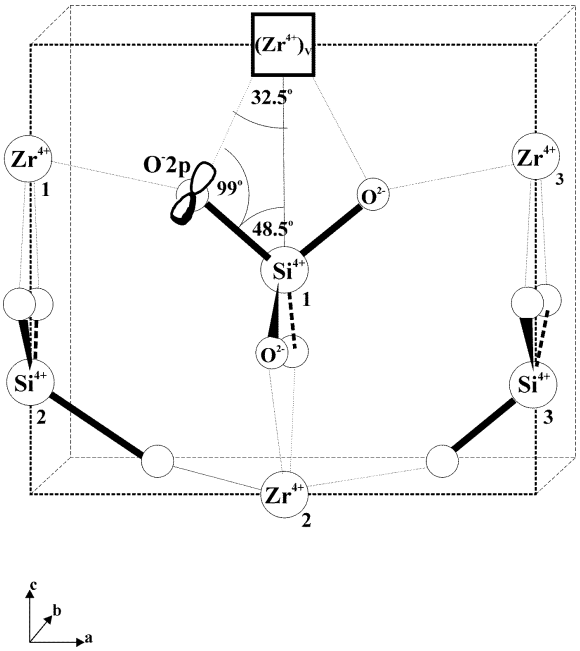

Figure 3. Model for the C centre. The figure depicts the ac-plane of the zircon lattice. For clarity not all atoms are shown. In the coordinate system of table 1 and with Si(1) as origin the $[r\theta\phi]$ coordinates of the atoms depicted are: Zr(vac) [299, 0, 0], Zr(1) [363, 65.6, 180], Zr(2) [299, 180, 0], O(1)(hole) [162, 48.5, 180].

The C centre appears after low temperature x-irradiation followed by warming of the crystal to RT, whereby the major low temperature electron and hole centres, the $Zr^{3+}(\alpha)$ centre and the $[AlO_4]^0$ centre, anneal out [1–4]. The C centre, once formed, is very stable. It appears that an electron or hole may have been captured at a site with lower energy than the low temperature centres.

An electron could be trapped at an O^{2-} vacancy (similar to an F centre in an alkali halide). Such a model of the C centre would require hf interactions with more than one Zr and/or Si neighbours and must be rejected.

A hole could be trapped at an oxygen of the SiO_4 groups. The hole might be expected to be in an oxygen $2p_\sigma$ orbital with a principal direction of the hf tensor along the bond direction, which is approximately as observed. However, the ratio of the isotropic to the anisotropic interaction in such a case is typically $a/b = 5$–6 and not the $a/b = 20$ observed here (see [7], chapter 7). The absolute values would be expected to be an order of magnitude higher, as a simple estimate shows by orthogonalizing an oxygen $2p_\sigma$ orbital to the Si^{4+} core orbitals ([7], chapter 7). Using an O^-–Si^{4+} distance of 162 pm we obtain $a/h = -242$ MHz and $b/h = -38$ MHz. Further, such a hole centre would not be particularly stable, as known from the way O^- hole centres in zircon decay [1–3].

In order to explain the observations and the stability of the C centre we propose that the C centre is a 2p hole in an oxygen of the SiO_4^{4-} group with the 2p hole orbital being almost perpendicular to the O–Si bond and directed towards a neighbouring Zr^{4+} vacancy (see figure 3). The fourfold negative Zr^{4+} vacancy represents a strong Coulomb attraction for the 2p O^- hole orbital. The ground state is expected therefore to be much lowered with respect to other O^-2p orientations resulting in a strong orbital quenching effect, thus explaining the

almost pure spin magnetism of the C centre with $g = 2$ and isotropic. The larger of the two observed hf interactions is with the nearest covalently bonded Si atom of the SiO_4 group. The hf interaction is dominated by exchange polarization effects, since the Si atom is almost in a nodal plane of the O^-2p hole orbital. In this geometry there is almost zero overlap between the oxygen 2p hole orbital and the Si core and consequently there is no direct 'positive' hf interaction. (Note, however, that a positive hf interaction would cause a negative hf interaction constant because of the negative nuclear moment of Si). Such a situation has been observed before for several oxygen hole centres in Al_2O_3, Na beta-alumina, GeO_2, SiO_2 and other oxides [8–11]. In these cases the hf interactions showed two distinct peculiarities: the isotropic hf constant a/h was negative (assuming $g_n > 0$) and the anisotropic hf constant b/h was much smaller than the value one would expect from classical dipole–dipole interactions between the unpaired hole and the magnetic nuclei involved (Al, Ge or Si).

The absolute signs of the hf constants a/h and b/h could not be determined from the EPR experiments. However, the analysis of the spectra showed that both have the same sign. Thus, since the classical dipole–dipole interaction has the opposite sign to a and b due to exchange interaction, the latter must be dominating and overcompensating the classical dipole–dipole interaction.

A semi-empirical model of the exchange polarization mechanism of transferred hf interactions was developed in [12] to explain the hf interaction of oxygen hole centres in the various oxides mentioned above. This theory explained the experimental data reasonably well quantitatively. The theory has been adapted in an approximate form for the present case of the C centre and estimates of a/h and b/h for Si interaction have been made. If the Si is strictly in the nodal plane of the 2p hole orbital then $a = a_{pol}$, where a_{pol} is the 'negative' spin density induced by exchange polarization. The anisotropic hf constant is given by the sum of two terms: $b = b_{pol} + b_{dd}$, where the first term is again due to exchange polarization and the second to the classical dipole–dipole interaction, which can be estimated approximately from the interaction between two point dipoles. However, the 2p hole orbital will be oriented towards the centre of the Zr^{4+} vacancy and consequently the axis of the 2p orbital will not be exactly perpendicular to the O^-–Si bond. Neglecting relaxation of the lattice, this angle is, in the ideal geometry, 99°. Using this angle in the calculation shows that there will be a small contribution of transferred hf interaction from the 2p hole orbital component parallel to the O^-–Si direction.

An estimate of the hf interaction can be derived from the following:

$$a = a_{overlap} + a_{pol} \tag{1}$$

$$b = b_{overlap} + b_{pol} \tag{2}$$

$$a_{overlap} = \tfrac{2}{3}\mu_0 g_e g_n \beta_e \beta_n |\Psi(0)|^2 \tag{3}$$

$$b_{overlap} = \frac{\mu_0}{8\pi} g_e g_n \beta_e \beta_n \int \frac{3z^2 - r^2}{r^5} |\Psi(r_n)|^2 \, \mathrm{d}V. \tag{4}$$

The constants μ_0, g_n, g_e, β_n and β_e are the permittivity of free space, the nuclear and electronic g-factors and the nuclear and Bohr magnetons respectively. $a_{overlap}$ and $b_{overlap}$ are the transferred hf interactions calculated in the usual one particle approximation with an oxide $2p_\sigma$ orbital (that is the component along the O^-–Si bond) orthogonalized to the Si^{4+} core (see [7], chapter 7). $b_{overlap} = b_{dd}$, if the one particle wavefunction is approximated by a δ-function at the hole site, i.e. approximating the magnetic moment of the hole by a point dipole. Rough estimates of $a_{overlap}$ and $b_{overlap}$ were made by approximate scaling of the terms in the expressions previously derived for the Al^{3+}–O^- exchange interactions (see equations (10) and (17) in [11]) by the ratios of the nuclear g-factors, $|\Psi(0)|^2$, or $\int (3z^2 - r^2)/r^5 |\Psi(r_n)|^2 \, \mathrm{d}V$ and the overlap integrals $|\langle \Psi, m_s \mid O^-, 2p_\sigma \rangle|^2$ or $|\langle \Psi, mp_\sigma \mid O^-, 2p_\sigma \rangle|^2$ for the Al^{3+} and the Si^{4+}

(where m denotes the quantum number of the orbital of the ion and p_σ is the orbital which has its axis along the O^-–Si bond.)

The results of the above calculations are given in table 3. Setting $\alpha = 90^\circ$ (where α is the angle between the 2p hole orbital and the O^-–Si^{4+} bond) and assuming no relaxation of the lattice, the magnitudes of a/h and b/h are calculated to within a factor of 2 and the ratio of $a/b = 16.4$, near the experimental value of 20. (The slight deviation from uniaxial symmetry of the Si hf tensor (see table 1) was neglected.) Setting the orientation of the 2p hole towards the Zr^{4+} vacancy and assuming no lattice relaxation (that is setting $\alpha = 99^\circ$) the results are closer to the experimental values. In view of the very crude approximations used (both a_{pol} and b_{pol} were calculated in an approximation in [12], and in the present calculations the approximation is even cruder because of the simple scaling procedure used) the agreement with experiment is quite remarkable. One could probably obtain a better agreement by allowing the O^- to relax towards the vacancy. However, in view of the approximate character of the estimate we have refrained from doing this. The measured orientation of the hf tensor does not exactly coincide with the regular O^-–Si bond direction in the zircon lattice (figure 3). This probably does indicate a relaxation of the O^- towards the Zr^{4+} vacancy, which would be expected to happen on the grounds of the electronic attractive force between the O^- and the negative Zr vacancy.

As seen from figure 3 there is one Zr^{4+} ion near the oxygen 2p hole (labelled 1 in figure 3) and another Zr^{4+} ion further away (labelled 2 in figure 3). The experimental Zr hf interaction constants are an order of magnitude smaller than those for Si, but the hf tensor is more anisotropic ($a/h = \pm 1.47$ MHz, $b/h = \pm 0.164$ MHz and $b'/h = \mp 0.13$ MHz). The largest hf interaction is in a plane perpendicular to the plane which contains the Zr^{4+} ion labelled 1 and the O^-–Si^{4+} bond (the ac-plane of the crystal, see figure 3 and table 1). The value of b'/h, describing the deviation of the hf tensor from uniaxial symmetry, is of about the same magnitude as b/h, but has the opposite sign. We assign the observed Zr hf interaction to the Zr labelled 1 in figure 3. Since there is no core overlap between Si^{4+} and Zr(2) it seems implausible to explain a transfer effect of polarization spin density from Si^{4+} to Zr(2). Even for an overlap integral of 0.1 (which is the magnitude of the $\langle O^- 2p_\sigma \mid Si^{4+} 2s \rangle$ in zircon) there would be only 1/100 of the spin density of Si at Zr(2). The observed value of a/h is at least an order of magnitude larger compared to what could be expected from overlap transfer effects. On the other hand, the hf data when assigned to Zr(1) show also effects of exchange polarization. The classical point dipole–dipole interaction for the regular Zr(1)–O separation of 213 pm $b_{dd}/h = 0.76$ MHz is larger than the observed value of $b_{exp}/h = 0.16$ MHz. The orientation of the tensor at least qualitatively points to the fact that the exchange polarization overcompensates the classical anisotropic interaction along the Zr(1)–O^- direction resulting in the observed tensor orientation. Unfortunately, we do not have adequate wavefunctions for the Zr^{4+} to be able to calculate a similar estimate for the polarization effects as has been done for Si^{4+}.

In summary, the proposed model explains the hitherto puzzling features of the C centre.

4.2. Structural model for the Z centre

The new experimental measurements on the Z centre now show clearly that it is due to a Cr^{3+} impurity, which must have been introduced during the crystal growth, probably from the lithium molybdate/molybdenum oxide melt. The reagents used were of high purity and did not list chromium as an impurity. The heavy metal and Fe^{3+} content was stated to be $<0.001\%$. One can discuss two sites for the Cr^{3+} ion: either a Zr^{4+} site or an Si^{4+} site. Since we observe hf interaction (i.e. superhyperfine interaction) with two equivalent Zr nuclei and no site splitting (except for possibly a very small site splitting which may manifest itself in a increased line

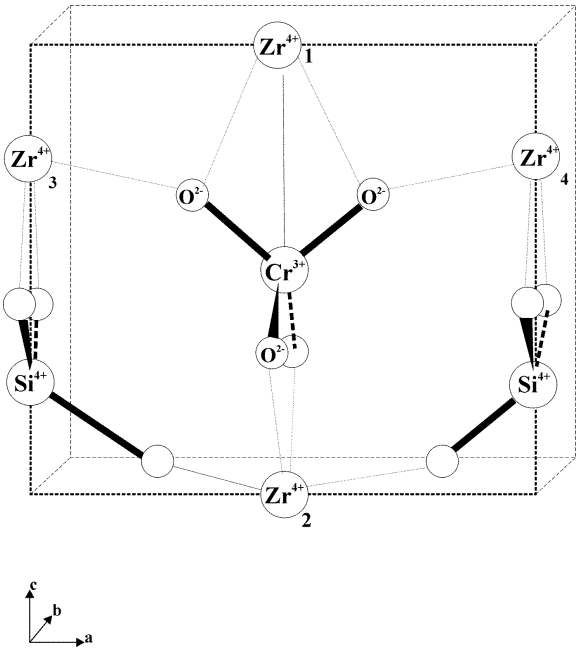

Figure 4. Model for the Z centre. Not all atoms are shown.

width when rotating the magnetic field away from the c-axis), the assignment has to be made to the Si^{4+} site (see figure 4). As this centre is not observed in a non-irradiated crystal we must presume that the chromium goes into the lattice as Cr^{4+} in the Si^{4+} site by donating its outer electrons into the covalent bonding with oxygens. After irradiation and annealing the Cr^{4+} captures an electron possibly from decay of the $Zr^{3+}(\alpha)$ centre formed at low temperature. The Cr^{4+} evidently provides a deeper electron trap than Zr^{4+}.

It is noted that Cr^{4+} is not necessarily EPR silent and, for example, EPR signals for both coexisting Cr^{4+} and Cr^{3+} have been observed in Al_2O_3 [13] and in forsterite (Mg_2SiO_4) [14]. Cr^{4+} often substitutes into tetrahedral sites when the lowest orbital state, a singlet, has threefold spin degeneracy, $S = 1$ (see Abragam and Bleaney [15] for details). Typically the zero field splittings are large, $\sim 8\ cm^{-1}$ in Al_2O_3 [13], when the spin doublet and spin singlet of the triplet state are widely separated. The only transition observable by EPR at conventional frequencies is that within the doublet with $M_S = \pm 1$ labels. For the conventional EPR configuration, $\boldsymbol{B}_1 \perp \boldsymbol{B}$, this transition has strictly zero transition probability in exactly uniaxial symmetry but becomes non-zero for small E- (doublet ZFS $= 2E$) values which may arise from distortion or strain [15]. There is apparent a small departure from uniaxial symmetry for the Z centre as evidenced from the fitted g-values (rhombic component, $c = |g_1 - g_2|/2 = 0.000\,45$ from table 2) but this is not such as to produce site splittings although, as already noted (see also [4]), the lines broaden considerably in non-axial orientations. We are currently carrying out further experiments on Cr-doped crystals in the hope of clarifying some of these aspects. To date no signals have been observed which could be assigned unambiguously to Cr^{4+}.

A salient feature of the data is the very large uniaxial zero field splitting parameter of approximately 1.5 T (in units $1/g_e\beta_e$). Although Cr^{3+} has been observed before with rather large values of $D/g_e\beta_e$, the value obtained here is unusually high, probably due to the strong crystal field along the c-axis from the two Zr^{4+} ions at a distance of 299 pm from the Cr^{3+} ion.

Large values of $D/g_e\beta_e$ for Cr^{3+} have also been observed in various oxides such as GeO_2, TiO_2, SnO_2 and TeO_2, where Cr^{3+} substitutes for the fourfold positively charged metal ion ([16], table 1). The situation in these oxides seems analogous to the present case. For example, in TeO_2, Cr^{3+} is bonded to four oxygens (two short and two long bonds, resulting in a slight deviation from uniaxial symmetry of the fine structure tensor) and has a positively charged Te ion above and below it along the [1 0 0] axis. For TeO_2 $D/g_e\beta_e$ is found to be 0.77 T [16]. Because of covalency, the Te atom carries fewer than four positive charges and it is well removed from Cr^{3+} (761 pm) in contrast to the situation in zircon where the Zr^{4+} is purely ionic and is at a distance of 299 pm from the Cr^{3+} ion. Thus qualitatively, a larger $D/g_e\beta_e$ value can be expected in zircon. Further, due to the effective negative charge of the Cr^{3+}, Coulombic forces may cause the two Zr^{4+} ions along the c-axis to relax inwards towards the Cr^{3+} to cause the high field necessary to explain the observed zero field splitting. Only weak repulsion is expected by the electronic cores because of the tetragonal orientation of the Cr^{4+}–O_4 bonds.

The chromium hf interaction of $A_\parallel/h = 45$ MHz (1.58 mT) is approximately the same as observed in many other cases including TeO_2 [16] and Al_2O_3 [13]. Breaking the hf matrix into its isotropic and anisotropic components, we obtain $a/g_e\beta_e = 1.30$ mT and $b/g_e\beta_e = -0.14$ mT. As observed for Cr^{3+} in Al_2O_3 [13], the isotropic contribution is dominant and can be attributed almost entirely to core polarization [15]. Experimentally the hyperfine field at the ^{53}Cr nucleus is $a/g_n\beta_n = -16.25$ T. After allowing for a small orbital contribution of -0.46 T [15] the net field at the nucleus arising from core polarization is -15.79 T. This is some 15% less than in Al_2O_3 [13] and perhaps as much as 40% below the free ion value as estimated from the average of that calculated for the isoelectronic ions V^{2+} and Mn^{4+} [15].

It is noted in conclusion that, although it is frequently necessary to postulate the presence of charge compensating ions, perhaps located remotely from the paramagnetic species being observed by EPR, in no case have we ever observed EPR evidence of such charge compensators.

5. Conclusion

The new EPR measurements have shown that the 'unusual' centres C and Z in zircon [4] are not coupled by a ferrimagnetic interaction as previously proposed but represent individual centres with high thermal stability. The C centre is a hole trap centre where the hole is located at an oxygen of the SiO_4^{4-} group oriented towards and stabilized by a nearest neighbour Zr^{4+} vacancy. The observed g-values and hf interactions with one Zr and one Si are explained in terms of practically complete orbital quenching and by the effects of exchange polarization dominating the Si and the Zr hf interactions. The Z centre is a Cr^{3+} impurity in an Si^{4+} site and thus an electron trap centre. The observed very large zero field splitting, $D/g_e\beta_e$ is due to the large crystal field along the c-axis, whereby the two Zr^{4+} ions probably relax towards the Cr^{3+}.

Acknowledgments

The authors acknowledge the support from the New Zealand–Federal Republic of Germany Science and Technological Agreement that has made this cooperation possible. Support from the Deutsche Forschungsgemeinschaft and the New Zealand Lotteries Commission is also acknowledged.

References

[1] Claridge R F C, Mackle K M, Sutton G L A and Tennant W C 1994 *J. Phys.: Condens. Matter* **6** 3429–36
[2] Claridge R F C, Mackle K M, Sutton G L A and Tennant W C 1994 *J. Phys.: Condens. Matter* **6** 10 415–22

[3] Claridge R F C, McGavin D G and Tennant W C 1995 *J. Phys.: Condens. Matter* **7** 9049–60
[4] Claridge R F C, Sutton G L A and Tennant W C 1997 *J. Magn. Reson.* **125** 107–13
[5] Chase A B and Osmer J A 1966 *J. Electrochem. Soc*. **113** 198–9
[6] Pilbrow J R 1978 *J. Magn. Reson.* **31** 479–90
[7] Spaeth J-M, Niklas J R and Bartram R H 1992 *Structural Analysis of Point Defects in Solids* (Berlin: Springer)
[8] Barklie R C, Niklas J R, Spaeth J-M and Bartram R H 1983 *J. Phys. C: Solid State Phys.* **16** 579–90
[9] Stapelbroek M, Bartram R H, Gilliam O R and Madacsi D P 1976 *Phys. Rev.* B **13** 1960–6
[10] Nuttall R H D and Weil J A 1981 *Can. J. Phys.* **59** 1696–708
[11] Stapelbroek M, Gilliam O R and Bartram RH 1977 *Phys. Rev.* B **16** 37–43
[12] Adrian F J, Jette A N and Spaeth J-M 1985 *Phys. Rev.* B **31** 3923–31
[13] Hoskins R H and Soffer B H 1964 *Phys. Rev.* **133** A490–3
[14] Whitmore M H, Sacra A and Singel D J 1993 *J. Chem. Phys.* **98** 3656–64
[15] Abragam A and Bleaney B 1970 *Electron Paramagnetic Resonance of Transition Ions* (Oxford: Clarendon)
[16] Watterich A, Raksányi K, Gilliam O R, Bartram R H, Kappers L A, Söthe H and Spaeth J-M 1992 *J. Phys. Chem. Solids* **53** 189–95